# Effect of the acid activation on a layered titanosilicate AM-4: The fine-tuning of structural and physicochemical properties

Maria N. Timofeeva [1,2*], Galina O. Kalashnikova[3], Kristina I. Shefer[1], Elena A. Mel'gunova[1], Valentina N. Panchenko [1,2], Anatoliy I. Nikolaev[3], Antonio Gil[4,*]

[1] *Boreskov Institute of Catalysis SB RAS, Prospekt Akad. Lavrentieva 5, 630090, Novosibirsk, Russian Federation*

[2] *Novosibirsk State Technical University, Prospekt K. Marksa 20, 630092, Novosibirsk, Russian Federation*

[3] *Nanomaterials Research Center, Kola Science Center, the Russian Academy of Sciences, 14 Fersman Street, Apatity 184209, Russia*

[4] *INAMAT-Science Department, Public University of Navarra, 31006 Pamplona, Spain*

**Corresponding authors**

M.N. Timofeeva

Tel.: +7-383-330-7284

Fax: +7-383-330-8056

E-mail: timofeeva@catalysis.ru

Address: Boreskov Institute of Catalysis SB RAS, Prospekt Akad. Lavrentieva 5, 630090, Novosibirsk, Russian Federation

A.Gil

Tel.: +34-948-169602

E-mail: andoni@unavarra.es

Address: Science Department, Los Acebos Building, Public University of Navarra,

Campus of Arrosadía, 31006 Pamplona, Spain

## Abstract

In this work we investigated the microporous layered titanosilicate AM-4 (Aveiro-Manchester material number 4) of a synthetic analogous the mineral Lintisite having edge-shared brookite-type $TiO_6$ chains. The objective of our work was to verify the effects of the acid activation on the AM-4 properties, treated with 0.0625-0.25M $HNO_3$. The results of the physicochemical characterization by SEM, XRD, IR and DR UV-vis spectroscopy, nitrogen adsorption/desorption at 77 K have provided evidences that texture, chemical composition, structural and physicochemical properties of AM-4 could be adjusted by treatment with 0.0625-0.25M $HNO_3$. According to the method of mass titration, surface acidity ($pH_{PZC}$) of AM-4 roses with increasing $HNO_3$ concentration, which was in accord with the increase of the reaction rate and yield of 1,5-benzodiazepine in the reaction of cyclocondansation between 1,2-phenylenediamine and acetone.

**Keywords:** Layered titanosilicate AM-4, Acid treatment, 1,5-benzodiazepine, 1,2-phenylenediamine, cyclocondensation reaction.

## 1. Introduction

Acidic modification of aluminosilicates is one of the methods for the synthesis of adsorbents and catalysts to produce materials with desired properties. Thus, acid treatment of zeolites leads to the removal of aluminum from zeolite frameworks. The appearance of lattice deficiencies due to the dealumination of zeolites can cause the formation of mesoporous channels in the zeolite crystal with 5-100 nm in pore diameter (Calsavara et al., 2000). Moreover, the acid treatment of zeolites can tune the acidity of zeolites, i.e. the concentration and strength of acid sites of the Brönsted type that is important for its catalytic application (Chen and Zones, 2010; Beyer, 2002; Fan et al., 2006). Textural and physicochemical properties of layered aluminosilicate materials also can be adjusted by acid treatment. Thus, chemical composition and physicochemical properties of clay materials, such as smectites, vermiculites, kaolinite, among others, can be adjusted by acid treatment (Komadel, 2016). For example, in the acid treatment of smectites, the protons of acid first replace the exchangeable cations ($Na^+$, $Ca^{2+}$, $Mg^{2+}$); after that they attack the layers and remove Al in the tetrahedral sheets (Komadel, 2016; Okada et al., 2006). Note that, such treatment of clay materials modifies its textural properties and/or amount of acid sites due to the disaggregation of clay particles, elimination of mineral impurities, changing the type of exchangeable cations.

According to the literature (Lv et al., 2007; Llabrés et al., 2003; Xiong et al., 2017; Lee et al., 2012; Tang et al., 2014) acid modification can be used both the change of properties of titanosilicates and its synthesis. Thus, the removal of the extra-framework $TiO_2$ without significantly affects the framework titanium species was demonstrated for the titatosilicate TS-1 with MFI zeolite structure after acid modification (Xiong et al., 2017). Such treatment leads to increasing amount of the active intermediate species Ti-OOH($\eta^2$) in oxidation processes. Moreover, the acid modification was used as one of the steps of the two-step post-synthesis strategy of Ti-Beta zeolite (Tang et al., 2014). In the first step, the dealumination of H-Beta zeolite to Si-Beta and formation of vacant T sites with associated silanol groups

proceeded due to the $HNO_3$ treatment. Then, vacant T sites in the Si-Beta zeolite reacted with the organometallic Ti complex $Cp_2TiCl_2$ and Ti species were incorporated into the framework of Beta zeolite upon the calcination.

The effect of the acid activation on the titanosilicate having –Ti-O-Ti-chains is the most interesting. For example, a microporous titanosilicate ETS-10 (ETS type, Engelhard titanosilicate) (Kuznicki, 1989) was modified with citric acid, $H_3PO_4$, $HNO_3$ (Lv et al., 2007) and HF (Llabrés et al., 2003). It was found that diluted acid solutions and short contact times did not lead to the crystal structure collapsing, also increasing the number of accessible titanium sites. Its amount was up to 2-3 times larger than in the parent material. It was suggested that acids mainly degrade the external surfaces of solid with the appearance of new Ti-OH groups.

Other examples of the titanosilicates having –Ti-O-Ti-chains is the lintisite-kukisvumite-group minerals and their synthetic analogous. Herein, we would like to draw your attention to AM-4 (Aveiro-Manchester material number 4, $Na_3(Na,H)Ti_2O_2[Si_2O_6]_2$ $2H_2O$) (Ferdov et al., 2014; Lin et al., 1997; Dadachov et al., 1997; Clearfield et al., 1997; Anderson et al., 1997). AM-4 is analogous to the mineral Lintisite discovered in the hyperalkaline pegmatites of Mount Alluaiv (the north-western part of the Lovozero massif, Kola peninsula) (Merlino et al., 1990). This material has a unique layered structure. According to Dadachov et al. (Dadachov et al., 1997), the structure of AM-4 consists of $TiO_6$ octahedra and $SiO_4$ tetrahedra. These two structural units connect to layers which consist of a sandwich of $SiO_4$:$TiO_6$:$SiO_4$:$TiO_6$:$SiO_4$ (**Fig. 1, Supporting Information (SI)**). The edge-sharing $TiO_6$ octahedra form the chains along (100), which are connected with each other via corner-sharing with $SiO_4$ tetrahedra. Sodium cations and water molecules are located in the interlamellar space (exchangeable) and in the space within the layer (structural cations). Because of the excellent cation-exchange properties, AM-4 has been reported as adsorbent for $Ag^+$, $Zn^{2+}$, $Cu^{2+}$ (Perez-Carvajal et al., 2012; Oleksiienko et al., 2017), cesium and strontium

(Yakovenchuk et al., 2012; Oleksiienko et al., 2017) and radionuclides ($^{241}$Am and $^{236}$Pu) (Oleksiienko et al., 2017; Al-Attar et al., 2003). Recently, AM-4 was demonstrated to be used as a solid base catalyst for the aqueous phase isomerisation of glucose, the condensation of benzaldehyde with ethyl acetoacetate (the Knoevenagel reaction) (Lima et al., 2008) and the synthesis of 2-methoxy-propanol-1 from methanol and propylene oxide (Timofeeva et al., 2019). Noteworthy that AM-4 in acid media transforms into layered protonated titanosilicate L3 (**Fig. 1, SI**) that may serve as a precursor for the synthesis of novel titanosilicate nanomaterials. In spite of the studies mentioned above, a systematic investigation of the acid activation of AM-4 lacks in the literature. The increasing interest in looking for new applications of AM-4 provokes a systematic study of this process. For this reason, our target in this work is to investigate the behavior of AM-4 under acid treatment with $HNO_3$ of several concentrations.

## 2. Experimental

### *2.1. Materials*

*Synthesis of AM-4.* The layer titanosilicate AM-4 was synthesized from powder of ammonium sulfate oxytitanium $(NH_4)_2TiO(SO_4)_2 \cdot H_2O$ (the product of loparite concentrate reprocessing (PJSC PhosAgro, Russia)), $Na_2SiO_3 \cdot 5H_2O$ (Neva Reactive) and NaOH (Merck). Hydrothermal synthesis of layer titanosilicate was carried out in a Teflon-lined autoclave with an inner volume of 450 $cm^3$. The synthesis was based on the consecutive transformations:

Ammonium sulfate oxytitanium → Natisite → Sitinakite → AM-4.

Stage 1 (Synthesis of natisite, $Na_2TiO(SiO_4)$): Ti,Si-gel was prepared by the mixing of 52.61 g of $(NH_4)_2TiO(SO_4)_2 \cdot H_2O$, 85.48 g of $Na_2SiO_3 \cdot 5H_2O$, 28.22 g of NaOH, and 317 g of

distilled water. The molar ratio of $Na_2O:SiO_2:TiO_2:H_2O$ was 5.6:3.1:1:130.4. This mixture was stirred at 298 K for 3 h.

Stage 2 (Synthesis of sitinakite**,** $Na_3Ti_4Si_2O_{13}(OH)\cdot 2H_2O$): The resulting mixture was transferred to an autoclave for further reaction. The temperature and time of reaction were modified from time to time. First step: autoclave was kept motionless at 503 K for 15 h, then was cooled down to 423 K for 2 h and was kept under stirring for 4 h. The second step (all the following procedures were under stirring): autoclave was heated up to 503 K and the mixture was aged in the autoclave for 64 h. Then, the autoclave was cooled down to 373 K for 2 h and was kept for 3 h. Third step: the autoclave was heated up to 503 K for 1 h and then quickly was cooled down to room temperature.

Stage 3 (Synthesis of AM-4, $Na_3(Na,H)Ti_2O_2[Si_2O_6]_2\ 2H_2O$): The obtained compound was separated by filtration, followed by repeated washing with distilled water and subsequent dryness at 333-343 K for 24 h. The yield of solid was 45 g.

*Modification of AM-4 with* $HNO_3$. 1 g of solid was suspended in 10 $cm^3$ of aqueous solutions of 0.0625 – 0.25 M of $HNO_3$ and the mixture was stirred at room temperature for 30 min. Then, the solid was separated, washed with water and dried at room temperature.

*2.2. Instrumental measurements*

The chemical analyses of the solids were carried out by means of inductively coupled plasma-atomic emission spectrometry (ICP-AES). The diffraction images were obtained with the use of a Thermo ARL X'tra device, with a non-monochromated Cu Kα radiation (λ = 1.5418 Å), focusing geometry θ-θ in the scanning mode within the range of angles from 3 to 75º, with a step of 0.05°.

The textural properties of the samples were determined from adsorption of $N_2$ at 77 K using an ASAP 2020 Plus Instrument from Micromeritics. The specific surface area ($S_{BET}$) was calculated from the adsorption data over the relative pressure range between 0.05 and 0.20. The total pore volume ($V_\Sigma$) was evaluated at a relative pressure $p/p_0$ of 0.99.

Morphology of samples was studied by SEM analysis using a JSM-6460LV (JEOL) field-emission scanning electron microscope

DRIFT spectra were recorded on a Shimadzu FTIR-8300S spectrometer with a DRS-8000 diffusion reflectance cell in the 400 - 6000 $cm^{-1}$ range with a resolution of 4 $cm^{-1}$. The DR-UV-vis spectra were recorded on a UV-2501 PC Shimadzu spectrometer with a IRS-250A accessory in the 190-900 nm range with a resolution of 2 nm, on samples in powder form placed into a special cell for DR-UV-vis measurement. $BaSO_4$ was used as a standard for measurements.

*2.3. Investigation of surface acidity of AM-4 samples*

The point of zero charge of AM-4 samples ($pH_{PZC}$) was determined by mass titration described in the literature (Subramanian et al., 1988). A pH meter was calibrated using pH 1.68 and 6.86 buffers. All measurements were carried out using distilled-deionized water.

The reaction of 1,2-phenylenediamine (I) with acetone was carried out at 323 K in a jacketed glass reactor (10 mL) equipped with a magnetic stirrer and connected to a thermostat. Methanol was used as a solvent. The standard procedure was as follows: 0.1 mmol of (I), 4 mL of methanol, 2.5 mmol of acetone, and 10-30 mg of a catalyst were added into the reactor. At various time intervals, aliquots were taken from the reaction mixture and analysed by GC and GC-MS analysis.

## 3. Results and discussion

### *3.1. The change of chemical composition of AM-4 after treatment with $HNO_3$*

***Chemical analysis.*** The chemical composition of AM-4 modified with 0.0625-0.25 M $HNO_3$ is shown in **Table 1**. According to the chemical analysis, the amount of $Na^+$ decreases with increasing acid concentration (**Fig. 1**). After the treatment of AM-4 with 0.0625 M and 0.25M $HNO_3$, the amount of $Na^+$ decreased by 72.7 and 97.9 %, respectively. Based on the changing of $Na^+$ concentration and structure of AM-4 (Lin et al., 1997; Dadachov et al., 1997), we can suggest that Na(2) and Na(3) located into in the interlayer space (**Fig. S1, SI**) are easily

replaced by protons first in the course of modification with 0.0625-0.25M $HNO_3$. At the same time, the high acid concentration will favour the change of Na(1) located in small cages (**Fig. S1, SI**)

***IR spectroscopic studies*.** The change of the chemical composition of AM-4 also was confirmed by DRIFT spectroscopy. The mid-infrared absorption spectra (400-1800 $cm^{-1}$) of AM-4 pristine and after acid modification are shown in **Fig. 2**. The spectrum of AM-4 shows broad bands in the regions of 400-700 $cm^{-1}$ and 700-1200 $cm^{-1}$, which can be attributed to the vibrations of the T-O bending modes and the asymmetric and symmetric stretching vibrations of the framework $TO_4$ polyhedra (Flanigen et al., 1974).

The treatment of AM-4 with $HNO_3$ leads to a shift of band assigned to Si-O mode (Lv et al., 2007; Ni et al., 2016; Ma et al., 2005; Kusabiraki, 1987) from 1129 to 1158 $cm^{-1}$. This blue shift is the result of the leaching sodium ions and the weakening strength of the Si-O bonds by the electrostatic interaction of protons in the vicinity of the framework anionic oxygen. In general, the intensities and width of all bands significantly increase that also indicates shortening of the interlayer distance. The bands in the 800-900 $cm^{-1}$ region observed in all spectra can be assigned to the normal modes including the $\nu(SiO_3)$ and the $\nu$(Ti-O) vibrations (Du et al., 1996; Camblor et al., 1993). Thus, the band at 912 $cm^{-1}$ may be attributed to the locally antisymmetric $\nu_{as}(SiO_3)$ mode. After acid modification, a shoulder at 830 $cm^{-1}$ appears in the spectra which can be due to the vibrations of the Ti-O and Si-O bond (Du et al., 1996; Camblor et al., 1993). The intensity of this band raises with increasing acid concentration. Note that all spectra also demonstrate a characteristic band at 967 $cm^{-1}$ that is attributed to a collective vibration of the Si-O-Ti bond or Si-O bond perturbed by the presence of Ti atoms in the framework of Tis. The change in structure follows also from a shift of band from 663 to 715 $cm^{-1}$ assigned to Si-O-T (where T = Si or Ti) stretching modes (**Fig. 2**). We can assume that this shift is due to the formation of hydroxyl groups (Si-OH and Ti-OH) (Lv et al., 2007). The bands at 1665 and 1710 $cm^{-1}$ due to the $\nu$(H-OH) mode of chemisorbed $H_2O$ on Ti and Si active sites (Panayotov et al.,

2005; Abdullah et al., 2016) are observed in the spectrum of AM-4. After modification with acid, the spectrum shows a band at 1636 $cm^{-1}$ corresponding to the overtone stretching of isolated Si-OH and Ti-OH groups ($2\nu_{OH}$), and a band at 1865 $cm^{-1}$ corresponding to the combination band ($\nu_{OH}$ $\delta_{OH}$) of adsorbed water (Dellarocca et al., 2001).

***DR-UV-vis spectroscopic studies.*** DR-UV-vis spectra of AM-4 pristine and after treatment with $HNO_3$ are shown in **Fig. 3**. The spectrum of AM-4 is characterized by an absorbance peak in the region of 240 - 280 nm. Moreover, a small shoulder in the region lower than 240 nm is found. The band in the region of lower 240 nm is assigned to the charge transfer from $O^{2-}$ to $Ti^{4+}$ in the tetrahedral ($T_d$) framework Ti-sites (Wang et al., 2012; Moliner and Corma, 2014; Emdadi et al., 2017; Raimondi et al., 2000), which could be due to the defects on the surface of the solid. At the same time, a broad absorption at 240 - 280 nm is assigned to the charge transfer from $O^{2-}$ to $Ti^{4+}$ in an octahedral ($O_h$) coordination. The high intensity of the band in this region indicates that a major titanium species are present in octahedral coordination. The modification of AM-4 with $HNO_3$ results in a broadening and shift of the spectrum to 240 - 260 nm. In general, the intensities of the bands rise as the acid concentration was increased. Note that the intensity of the shoulder peak at < 240 nm is on the rise relative to the main peak. These findings can point out the removal of Ti with $O_h$ coordination and appearance of $T_d$ coordinated Ti due to the changes that are taking place in the structure of AM-4.

### *3.2. The change of structural and textural properties of AM-4 after treatment with $HNO_3$*

***XRD studies.*** X-ray diffractometry was used to analyze the changes in the structure of AM-4 occurring in the course of the acid activation. The X-ray diffraction patterns of the samples are shown in **Fig. 4** The unit cell parameters were estimated by the method of full-profile analysis (R = 11% in all cases) using X'Pert HighScore Plus Program (Version 2.1). As can be seen from **Table 2**, our results for AM-4 are in accord with that for AM-4 synthesized from $TiCl_3$ (Ferdov , 2014) and $TiCl_4$ (Dadachov et al., 1997). The acid treatment causes strongly changes in the XRD pattern of the sample (**Fig. 4**). Thus, the lowest reflection angle (200) shifts

from 5.94 to 7.46° (2θ). This shift and other changes point out the transformation of the structure. The sharply decreasing unit cell parameter *c* from 29.22 to 11.92 Å (**Table 2**) reflects the contraction of the unit cell that can be caused both by the incorporation of the protons into the framework, but also by the low of its effective radius. Note that the structural transformation of the Lintisite-Kukisvumite group in acidic solutions and the decreasing cell parameters were demonstrated by Yakovenchuk et al. (2012).

***Scanning electron microscopic study.*** The change of morphology and particle size of AM-4 after its modification with 0.25M $HNO_3$ was investigated by scanning electron microscope (SEM). One can be seen from **Fig. 5A-B**, pristine AM-4 is of the form the relatively uniform aggregates of rosette-like form with 7-8 μm of the width and 15-17 μm of the length. The rosette-like aggregates have a lamellar structure due to the aggregation of titanosilicate platelets. The thickness of titanosilicate platelets is 0.15-0.25 μm (**Fig. 5C**). Note that AM-4 with other kinds of morphologies has been reported in the literature (Lin et al., 1997; Perez-Carvajal et al., 2012). For example, using $TiO_2$ anatase as a Ti source, Perez-Carvajal et al. (2012) prepared AM-4 with sheet-like growth habit. Such shape AM-4 had layers of an average 1.2 μm length and thickness of 50 nm. Plate-like crystals of AM-4 prepared from $TiCl_4$ was demonstrated by Ferdov (2014). Therefore, we can suggest that the morphology of AM-4 is determined by the Ti source which affects the mechanism of aggregation of particles.

Modification of AM-4 with 0.25M $HNO_3$ for 30 min at room temperature leads to the change of particle size. The distribution of particles became inhomogeneous (**Fig. 6A**). The width and the length of particles vary from 3 to 5 and 5-17 μm, respectively (**Fig. 6B**). At the same time, the acid modification does not strongly affect the morphology of particles, however, the lamellar structure of the rosette-like aggregates get thinner due to the peeling of the titanosilicate platelets. Titanosilicate platelets are starting to get thinner; their thickness is in the region of 0.05-0.20 μm.

Perez-Carvajal et al. (2012) observed the swelling and exfoliation of AM-4 in the course of proton exchange with acetic and the following its acid intercalation with nonylamine. It is possible in our case. Thus, the changes in XRD patterns (**Fig. 4**), i.e. broaden and shift of signals in the 2 theta degree region of 25-40$^{o}$, can point to the swelling of AM-4 after its modification with $HNO_3$. Similar changes in XRD patterns were demonstrated for AM-4 modified with $Ag^{+}$, $Zn^{2+}$ and $Cu^{2+}$ ions by ion exchange (Perez-Carvajal et al., 2012). At the same time, the change in thickness of titanosilicate platelets can indicate the slight exfoliation of AM-4. At the same time, the change in thickness of titanosilicate platelets and the slight increase in the space between the titanosilicate platelets (**Fig. 6C**) can point to the slight exfoliation of AM-4.

***Textural properties studies***. The textural properties of AM-4 samples derived by $HNO_3$ treatment are estimated from nitrogen adsorption at 77 K. The adsorption isotherms are type II according to the international union of pure and applied chemistry (IUPAC) classification (Kruk and Jaroniec, 2001; Ma et al., 2009). Type II is typical of nonporous or macroporous (pore width > 50 nm) materials. The hysteresis loops developed after desorption of $N_2$ adsorbed can be related to type H3 that can be associated with slit-shaped pores or the space between parallel plates. The presence of macropores in such type of samples should be related to the intraparticle condensation of $N_2$ at 77 K. The treatment of AM-4 with 0.0625-0.25 M $HNO_3$ reduces to the enlargement of macropore size that is caused by the removal of the sodium ions from AM-4 framework and formation of defects ion the surface of solid.

The specific surface areas and the total pore volumes are given in **Table 1**. According to experimental data, the total surface area decreases in the order

0.25M AM-4 > 0.125M AM-4 > 0.0625M AM-4 > AM-4,

which also was along with the changing total pore volume. Remarkable, these trends are in agreement with SEM data, which point to the thinning titanosilicate platelets and the slight

increase the space between the titanosilicate platelets after AM-4 modification with acid (**Fig. 5-6**)

### *3.3. The change of surface acidity of AM-4 after treatment with $HNO_3$*

Physicochemical and catalytic approaches have been followed to monitoring changes in surface acidity of AM-4 modified with $HNO_3$.

***The method of mass titration***. The change of the surface acidity in the course of activation with $HNO_3$ was investigated by the method of mass titration in aqueous solution. This method was successfully used by Noh and Schwarz for determination of the point of zero charge ($pH_{PZC}$) of oxides and carbons modified by $HNO_3$ (Subramanian et al., 1988; Noh and Schwarz, 1990). The method is based on the addition of portions of solid to the water. The pH of the system will continue to changes and approach a constant value, which is the point of zero charge ($pH_{PZC}$). Plots of the mass percentage of AM-4 modified with $HNO_3$ versus pH are shown in **Fig. 1.** $pH_{PZC}$ was determined as the plateau in the mass titration curve. Based exactly on these data, a relation between the $pH_{ZPC}$ and the acid concentration was build **(Fig. 1).** The results of this relation point out that the surface acidity of AM-4 monotonically rises from 11.2 to 4.0 with increasing $HNO_3$ concentration from 0 to 0.25M. The variation of the surface acidity is due to the emergence of the Brønsted acid sites (BAS) which are formed in two ways. The first way is based on the replaced of sodium ions by protons. Another way is based on the coordination change of the Ti atoms upon hydration that following from Kataoka and Dumesic's model (Gao and Wachs, 1999). This model predicts that BAS are associated with Ti-O-Si bridges where the Ti atoms reside not in tetrahedral sites but in pentahedral or octahedral sites, regardless of composition. Adsorption of water can lead to the partial hydrolysis of the Ti-O-Si bridges to produce the $O_wH$ ($O_w$ is atom in the $H_2O$) and bridge -OH group (similar to bridging Si-(OH)-Al groups in zeolites), i.e. two types of Brønsted acid sites (Han et al., 2017). The bridge -OH groups possess stronger Brønsted acidity then the $O_wH$ and can act as a catalytic site. Lin et al. (1997) reported that surface hydroxylation is crucial to the presence of Brønsted acidity. It was

suggested that the positive charge on Si is balanced by a -OH group on Si, thus producing Brønsted acidity. However, another viewpoint was expressed by Contescu et al. (1995), who suggested that the acidic –OH groups might be located on a titanium surface ion. According to IR spectroscopic data (**Fig. 3**), -Si-OH and -Ti-OH groups are formed on AM-4 after modification with $HNO_3$. We can assume that both -Si-OH and -Ti-OH together with protons located in the interlayer space (**Fig. S1, SI**) can act as Brønsted acid sites.

***The catalytic method.*** Other confirmation of the change in surface acidity after AM-4 treatment with $HNO_3$ may be the reaction of the cyclocondensation between 1,2-phenylenediamine and acetone (**Scheme 1**) because the reaction rate and yield of 1,5-benzodiazepine rise with increasing strength and amount of acid sites (Tajbakhsh et al., 2006; Timofeeva et al., 2017). We investigated the effect of acid activation of AM-4 on reaction rate and yield of 1,5-benzodiazepine (III) in methanol as reaction medium considering an acetone/(I) molar ratio of 2.5 and at 323 K. According to experimental data, the main products were the 1,5-benzodiazepine (III) and intermediate product (II) which are formed due to the consecutive reactions (**Fig. S2, SI)**. Selectivities towards (II) and (III) also depended on the $HNO_3$ concentration (**Fig. 7A**). Selectivity towards (II) decreased with increasing $HNO_3$ concentration. Maximal selectivity towards (II) was 80.2% for 30 min of reaction in the presence of 0.0625M AM-4. At the same time, the increasing acid concentration led to increasing the selectivity towards (III).

The low performance was observed in the presence of AM-4, the conversion of 1,2-phenylenediamine was about 3% for 120 min. However, after AM-4 treatment with 0.25M conversion of 1,2-phenylenediamine improved. One can see from **Fig. 7A**, conversion of 1,2-phenylenediamine raises with increasing $HNO_3$ concentration. The comparison of the distribution of products at isoconversion of (I) (57.8-59.1%) pointed that selectivity towards (III) rose from 11.9 to 19.6% with increasing acid concentration from 0.0625 to 0.25M (**Table S1, SI**). Since the reaction takes place in two stages (I) → (II) → (III) (**Scheme 1**), this trend can indicate

that acid concentration also affects the reaction rate of the second stage that is in accord with the variation in the surface acidities. In general, the higher surface acidity favours the higher yield of (III) (**Fig. 7B**).

It was interesting to evaluate the efficiency of 0.25M AM-4 as an acid-type catalyst. It is with this aim in mind that we compared catalytic properties of 0.25M AM-4 with H-ZSM-5 (Si/Al 28, framework type MFI), β-zeolite (Si/Al 30, framework type BEA) (Tajbakhsh et al., 2006; Timofeeva et al., 2017), HY (Si/Al 2.5, framework type FAU), heulandite (Si/Al 5, framework type HEU) (Tajbakhsh et al., 2006), and Mt modified with 0.25M $HNO_3$ (0.25M Mt) (**Table 3**). The reaction was investigated at a 4/1 molar ratio of acetone/(I), 0.2/1.0 mass ratio of catalyst/(I) and 333 K under solvent-free conditions. It was found that the catalytic performance of the 0.25M AM-4 was higher as compared to the H-ZSM-5 and β-zeolite. At the same time, the efficiencies of 0.25M Mt and zeolites, such as HY and heulandite, were higher than those of 0.25M AM-4. Taking into account the microporosity of these samples, we can suggest that the difference of their activity is related to the surface acidity (amount and strength of acid sites) and accessibility to the active sites for the reactants. This suggestion is consistent with the difference in surface acidity ($pH_{PZC}$) of 0.25M AM-4 and 0.25M Mt (**Fig. S3, SI**) and the specific surface area of 0.25M AM-4 (30 $m^2/g$) and 0.25M Mt (112 $m^2/g$) samples.

## 5. Summary and conclusions

In this work we investigated titanosilicate layered material AM-4 that is related to the synthetic analogue of the natural Lintisite group. AM-4 was synthesized from ammonium sulfate oxytitanium $(NH_4)_2TiO(SO_4)_2 \cdot H_2O$ (the product of loparite concentrate reprocessing) and $Na_2SiO_3 \cdot 5H_2O$ as a source of Ti and Si, respectively. The synthesis of AM-4 was based on the consecutive transformations: ammonium sulfate oxytitanium → natisite → sitinakite → AM-4. The effect of the acid activation of AM-4 with 0.0625-0.25M $HNO_3$ on its chemical composition, structural, textural and acid-base properties was investigated. The results indicated that the acid-base properties of AM-4 can be adjusted through its treatment with $HNO_3$. It was found that after

the acid treatment, the chemical composition of the solid changed strongly due to the replacement of $Na^+$ located in the interlayer space by $H^+$. The acid treatment also produced changes in the textural properties. Specific surface area and total pore volume increased with increasing acid concentration. The method of mass titration was used for the analysis of the surface acidity ($pH_{PZC}$). The higher acid concentration was found to favour the rising surface acidity. It was suggested that both -Si-OH and -Ti-OH together with protons located in the interlayer space can act as Brønsted acid sites. The appearance of acid sites is confirmed by evidence from the investigation of catalytic properties of AM-4 samples in the reaction of the cyclocondansation between 1,2-phenylenediamine and acetone. The reaction rate and yield of 1,5-benzodiazepine rose with increasing surface acidity ($pH_{ZPC}$).

## Acknowledgments

This work was conducted within the framework of the budget projects AAAA-A17-117041710082-8 for Boreskov Institute of Catalysis and AAAA-A17-117020110075-1 for Nanomaterials Research Centre of the Federal Research Centre “Kola Science Centre of the Russian Academy of Sciences” (NMRC KSC RAS), respectively. AG thanks Santander Bank for funding through the Research Intensification Program.

## References


Abdullah, M., Kamarudin, S.K., Shyuan, L.K., 2016. $TiO_2$ nanotube-carbon (TNT-C) as support for Pt-based catalyst for high methanol oxidation reaction in direct methanol fuel cell. Nanoscale Res. Lett., 11, 553. https://doi.org/10.1186/s11671-016-1587-2

Al-Attar, L., Dyer, A., Harjula, R., 2003. Uptake of radionuclides on microporous and layered ion exchange materials. J. Mater. Chem. 13, 2963-2968. https://doi.org/10.1039/b308200h

Anderson, M.W., Ferreira, A., Rocha, J., Dadachov, M.S., 1997. *Ab initio* structure determination of layered sodium titanium silicate containing edge-sharing titanate chains (AM4) $Na_3(Na,H)Ti_2O_2[Si_2O_6]\cdot 2.2H_2O$. Chem. Commun. 2371-2372. https://doi.org/10.1039/a707106j

Beyer H.K., 2002. Dealumination Techniques for Zeolites. In Karge, H.G., Weitkamp, J. (Eds) Post-Synthesis Modification I. Molecular Sieves (Science and Technology). Springer, Berlin, Heidelberg, 203-255. https://doi.org/10.1007/3-540-69750-0_3

Calsavara, V., Machado, N.R.C.F., Bernardi Jr, J.L., Sousa-Aguiar, E.F., 2000. On the acidity and/or basicity of USY zeolites after basic and acid treatment. Brazilian J. Chem. Eng. 17, 91-98. https://dx.doi.org/10.1590/S0104-66322000000100008

Chen, C.-Y., Zones, S.I., 2010. Post-synthetic treatment and modification of zeolites. In Cejka, J., Corma, A., Zones, S. (Eds) Zeolites and Catalysis: Synthesis, Reactions and Applications, WileyVCH Verlag, 155-170. doi:10.1002/9783527630295.ch6

Clearfield, A., Bortun, A.I., Bortun, L.N., Cahill R.A., 1997. Synthesis and characterization of a novel layered sodium titanium silicate $Na_2TiSi_2O_7$ center dot 2H(2)O. Solvent Extr. Ion Exch. 15, 285-304 https://doi.org/10.1080/07366299708934479

Camblor, M.A., Corma, A., Perez-Pariente, J., 1993. Infrared spectroscopic investigation of titanium in zeolites. A new assignment of the 960 $cm^{-1}$ band. J. Chem. Soc., Chem. Commun. 557-559. https://doi.org/10.1039/C39930000557

Contescu, C., Popa, V.T., Miller, J.B., Ko, E.I., Schwarz, J.A., 1995. Proton affinity distributions of $TiO_2$-$SiO_2$ and $ZrO_2$-$SiO_2$ mixed oxides and their relationship to catalyst activities for 1-butene isomerization. J. Catal. 157, 244-258. https:// doi.org/10.1006/jcat.1995.1285

Dadachov, M.S., Rocha, J., Ferreira, A., Lin, Z., Anderson, M.W., 1997. *Ab initio* structure determination of layered sodium titanium silicate containing edge-sharing titanate chains (AM-4) $Na_3(Na,H)Ti_2O_2[Si_2O_6]\cdot 2.2H_2O$. Chem. Commun. 2371-2372 https://doi.org/10.1039/A707106J

Dellarocca, V., Marchese, L., Peña, M.L., Rey, F., Corma, A., Coluccia, S., 2001. Surface properties of mesoporous Ti-MCM-48 and their modifications produced by silylation. Stud. Surf. Sci. Catal**.** 140, 209-220. https://doi.org/10.1016/S0167-2991(01)80150-6

Du, H., Zhou, F., Pang, W., Yue, Y., 1996. Synthesis and characterization of titanium silicate molecular sieves with zorite-type structure. Micropor. Mater. 7, 73-80. https://doi.org/10.1016/0927-6513(96)00014-4

Emdadi, L., Tran, D.T., Zhang, J., Wu, W., Song, H., Gan, Q., Liu, D., 2017. Synthesis of titanosilicate pillared MFI zeolite as an efficient photocatalyst. RSC Adv. 7, 3249-3256. https://doi.org/10.1039/c6ra23959e

Fan Y, Bao X, Lin X, Shi G, Liu H., 2006. Acidity adjustment of HZSM-5 zeolites by dealumination and realumination with steaming and citric acid treatments. J. Phys. Chem. B 110, 15411-15416. https://doi.org/10.1021/jp0607566

Ferdov, S., 2014. Layered titanosilicates for size- and pattern-controlled overgrowth of MFI zeolite. Cryst. Eng. Comm. 16, 4467-4471. https://doi.org/10.1039/C3CE42644K

Flanigen, E.M., Khatami, H., Szymansky, H.A., 1974. Infrared structural studies of zeolite frameworks. Adv. Chem. 101, 201-229. https://doi.org/10.1021/ba-1971-0101.ch016

Gao, X., Wachs, I. E., 1999. Titania-silica as catalysts: molecular structural characteristics and physico-chemical properties. Catal. Today 51, 233-254. https://doi.org/PII: S0920-5861(99)00048-6

Han, L. Wen, C., Wu, Z., Wang, J., Chang, L., Feng, G., Zhang, R., Kong, D., Liu, J., 2017. Density functional theory investigations into the structures and acidity properties of Ti-doped SSZ-13 zeolite. Micropor. Mesopor. Mater. 237, 132-139. https://doi.org/10.1016/j.micromeso.2016.09.028

Komadel, P., 2016. Acid activated clays: Materials in continuous demand. Appl. Clay Sci. 131, 84-99. http://dx.doi.org/10.1016/j.clay.2016.05.001

Kruk, M., Jaroniec, M., 2001. Gas adsorption characterization of ordered organic-inorganic nanocomposite materials. Chem. Mater. 13, 3169-3183. https://doi.org/10.1021/cm0101069

Kusabiraki, K., 1987. Infrared and Raman spectra of vitreous silica and sodium silicates containing titanium. J. Non-Crystall. Solids 95, 411-418. https://doi.org/10.1016/s0022-3093(87)80138-2

Kuznicki, S.M., 1989. Large-pored crystalline titanium molecular sieve zeolites. US Pat. 4,853,202A

Lee, S.L., Nur, H., Wei, S. C., 2012. Effect of acid treatment on silica-titania aerogel as oxidative-acidic bifunctional catalyst. Appl. Mech. Mater. 110-116, 457-464. https://doi:10.4028/www.scientific.net/AMM.110-116.457

Lin, Z., Rocha, J., Brandao, P., Ferreira, A., Esculcas, A.P., Pedrosa de Jesus, J.D., 1997. Synthesis and structural characterization of microporous umbite, penkvilksite, and other titanosilicates. J. Phys. Chem. B 101, 7114-7120. https://doi.org/10.1021/jp971137n

Lima, S., Dias, A. S., Lin, Z., Brandao, P., Ferreir, P., Pillinger, M., Rocha, J., Calvino-Casilda, V., Valente, A.A., 2008. Isomerization of D-glucose to D-fructose over metallosilicate solid bases. Appl. Catal. A 339, 21-27. https://doi.org/10.1016/j.apcata.2007.12.030

Lv, L., Zhou, J. K., Su, F., Zhao, X. S., 2007. Local structure changes of microporous titanosilicate ETS-10 upon acid treatment. J. Phys. Chem. C 111, 773-778. https://doi.org/10.1021/jp056107w

Llabrés I Xamena, F.X., Calza, P., Lamberti, C., Prestipino, C., Damin, A., Bordiga, S., Pelizzetti, E., Zecchina, A., 2003. Enhancement of the ETS-10 titanosilicate activity in the shape-selective photocatalytic degradation of large aromatic molecules by controlled defect production. J. Am. Chem. Soc. 125, 2264-2271. https://doi.org/10.1021/ja027382o

Ma, J.G., Liu, Y.C., Xu, C.S., Liu, Y.X., Shao, C.L., 2005. Preparation and characterization of ZnO particles embedded in $SiO_2$ matrix by reactive magnetron sputtering. J. App. Phys. 97, 103509. https://doi.org/10.1063/1.1897493

Ma, T.Y., Zhang, X.J., Yuan, Z.Y., 2009. Hierarchical meso-/macroporous aluminum phosphonate hybrid materials as multifunctional adsorbents. J. Phys. Chem. C 113, 12854-12862. https://doi.org/10.1021/jp903412m

Merlino, S., Pasero, M., Khomyakov, A.P., 1990. The crystal structure of lintisite, $Na_3LiTi_2[Si_2O_6]O_2$ $2H_2O$, a new titanosilicate from Lovozero (USSR). Zeitschrift fur Kristallographie 193, 137-148. https://doi.org/10.1524/zkri.1990.193.1-2.137

Moliner, M., Corma, A., 2014. Advances in the synthesis of titanosilicates: From the medium pore TS-1 zeolite to highly-accessible ordered materials. Micropor. Mesopor. Mater. 189, 31-40. https://doi.org/10.1016/j.micromeso.2013.08.003

Ni. X., Xiang, M., Fu, W., Ma, Y., Zhu, P., Wang, W., He, M., Yang, K., Xiong, J., Tang, T., 2016. Direct synthesis of mesoporous zeolite ETS-10 and Ni-ETS-10 with good catalytic performance in the Knoevenagel reaction. J. Porous Mater. 23, 423-429. https://doi.org/10.1007/s10934-015-0096-5

Noh, J.S., Schwarz, J.A., 1990. Effect of $HNO_3$ treatment of the surface acidity of activated carbons. Carbon 28, 675-682. https://doi.org/10.1016/0008-6223(90)90069-B

Okada, K., Arimitsu, N., Kameshima, Y., Nakajima, A., MacKenzie, K.J.D., 2006. Solid acidity of 2:1 type clay minerals activated by selective leaching. Appl. Clay Sci. 31, 185-193. https://doi.org/10.1016/j.clay.2005.10.014

Oleksiienko, O., Wolkersdorfer, C., Sillanpa, M., 2017. Titanosilicates in cation adsorption and cation exchange – A review. Chem. Eng. J. 317, 570-585. http://dx.doi.org/10.1016/j.cej.2017.02.079

Perez-Carvajal, J., Lalueza, P., Casado, C., Tellez, C., Coronas, J., 2012. Layered titanosilicated JDF-L1 and AM-4 for biocide applications. Appl. Clay Sci. 56, 30-35. https://doi.org/10.1016/j.clay.2011.11.020

Panayotov, D.A.,' Yates Jr., J.T., 2005. Depletion of conduction band electrons in $TiO_2$ by water chemisorption – IR spectroscopic studies of the independence of Ti–OH frequencies on electron concentration. Chem. Phys. Lett. 410, 11-17. https://doi.org/10.1016/j.cplett.2005.03.146

Raimondi, M.E., Gianotti, E., Marchese, L., Martra, G., Maschmeyer, T., Seddon, J.M., Coluccia, S., 2000. A spectroscopic study of group IV transition metal incorporated direct templated mesoporous catalysts. Part 1: A Comparison between materials synthesized using hydrophobic and hydrophilic Ti precursors. J. Phys. Chem. B 104, 7102-7109. https://doi.org/10.1021/jp993545s

Subramanian, S., Noh, J.S., Schwarz, J.A., 1988. Determination of the point of zero charge of composite oxides. J. Catal. 114, 433-439. https://doi.org/10.1016/0021-9517(88)90046-2

Tang, B., Dai, W., Sun, X., Guan, N., Li, L., Hunger, M., 2014. A procedure for the preparation of Ti-Beta zeolites for catalytic epoxidation with hydrogen peroxide. Green Chem. 16, 2281-2291. https://doi.org/10.1039/c3gc42534g

Tajbakhsh, M., Heravi, M.M., Mohajerani, B., Ahmadia, A.N., 2006. Solid acid catalytic synthesis of 1,5-benzodiazepines: A highly improved protocol. J. Mol. Catal. A 247, 213-215. https://doi.org/10.1016/j.molcata.2005.11.033

Timofeeva, M.N., Prikhod'ko, S.A., Makarova, K. O., Malyshev, M.E., Panchenko, V.N., Ayupov, A.B., Jhung, S.H., 2017. Iron-containing materials as catalysts for synthesis of

1,5-benzodiazepine from 1,2-phenylenediamine and acetone. React. Kinet. Mech. Catal. 121, 689-699. https://doi.org/10.1007/s11144-017-1190-2

Timofeeva, M.N., Kurchenko, J.V., Kalashnikova, G.O., Panchenko, V.N., Nikolaev, A.I., Gil, A., 2019. A layered titanosilicate AM-4 as a novel catalyst for the synthesis of 1-methoxy-2-propanole from propylene oxide and methanol. Appl. Catal. A 587, 117240. https://doi.org/10.1016/j.apcata.2019.117240

Wang, J., Xu, L., Zhang, K., Peng, H., Wu, H., Jiang, J., Liu, Y., Wu, P., 2012. Multilayer structured MFI-type titanosilicate: Synthesis and catalytic properties in selective epoxidation of bulky molecules. J. Catal. 288, 16-23. https://doi.org/10.1016/j.jcat.2011.12.023

Xiong, G., Jia, Q., Cao, Y., Liu, L., Guo, Z., 2017. The effect of acid treatment on the active sites and reaction intermediates of the low-cost TS-1 in propylene epoxidation. RSC Adv. 7, 24046-24054. https://doi.org/10.1039/c7ra02983g

Yakovenchuk, V.N., Krivovichev, S.V., Pakhomovsky, Y.A., Selivanova, E.A., Ivanyu, G.Yu., 2012. Microporous Titanosilicates of the Lintisite Kukisvumite Group and Their Transformation in Acidic Solutions. In S.V. Krivovichev (Ed.) Minerals as Advanced Materials II, Springer-Verlag: Berlin Heidelberg, 229-238. https://doi.org/10.1007/978-3-642-20018-2_23

## Table caption

**Table 1**. Chemical composition and textural properties of AM-4 and AM-4 modified with $HNO_3$.

**Table 2**. Unit cell parameters for AM-4 pristine and modified with $HNO_3$.

**Table 3.** Reaction of 1,2-phenylenediamine with acetone in the presence of Brønsted type catalytic systems

**Table 1**. Chemical composition and textural properties of AM-4 and AM-4 modified with $HNO_3$.

| | Experimental conditions | | Chemical composition, (wt.%) | | | Si/Ti (mol/mol) | Textural properties | |
|---|---|---|---|---|---|---|---|---|
| | $HNO_3$ (mol/mL) | $HNO_3$/solid (mmol/g) | Na | Si | Ti | | $S_{BET}$ ($m^2/g$) | $V_\Sigma$ ($cm^3/g$) |
| AM-4 | - | - | 32.3±0.2 | 29.5±0.2 | 34.3±0.2 | 1.5 | 20 | 0.070 |
| 0.0625M AM-4 | 0.0625 | 3.125 | 8.8±0.1 | 33.1±0.2 | 54.2±0.2 | 1.1 | 27 | 0.082 |
| 0.125M AM-4 | 0.125 | 6.25 | 4.8±0.1 | 35.9±0.2 | 54.4±0.2 | 1.1 | 29 | 0.088 |
| 0.25M AM-4 | 0.25 | 12.5 | 0.7±0.1 | 37.2±0.2 | 54.5±0.2 | 1.1 | 30 | 0.095 |

**Table 2**. Unit cell parameters for AM-4 pristine and modified with $HNO_3$.

| Sample | *a* (Å) | *b* (Å) | *c* (Å) | β ($^0$) | Space group | Ref. |
|---|---|---|---|---|---|---|
| AM-4 | 5.197(7) | 8.54(1) | 29.22(5) | 91.0(1) | A2/a | This work |
| 0.0625M AM-4 | 5.21(1) | 8.76(2) | 11.94(1) | 100.78(8) | $P2_1/a$ | This work |
| 0.25M AM-4 | 5.21(2) | 8.66(5) | 11.92(4) | 100.49(5) | $P2_1/a$ | This work |
| AM-4 | 5.2012(8) | 8.573(2) | 29.300(6) | 89.26(1) | A2/a | (Dadachev et al., 1997) |
| AM-4 | 5.21(1) | 8.60(1) | 28.58(3) | 88.8(1) | A2/a | (Ferdov et al., 2014) |

**Table 3.** Reaction of 1,2-phenylenediamine with acetone in the presence of Brønsted type catalytic systems

| Catalyst | Structural properties | | | Catalytic properties [a] | | | Ref. |
|---|---|---|---|---|---|---|---|
| | Framework type | Pore size (Å) | Pore dimensionality | Time (min) | Yield of (III) (%) | W $10^3$ (mmol/h) | |
| 0.25M AM-4 | Clay's materials | 5.2 x 8.7<br>8.7x 8.7 | 2-D | 180<br>300 | 58<br>67 | 19.5<br>11.2 | This work |
| 0.25M Montmorillonite | Clay's materials | 3.3 | 2-D | 120<br>180 | 83<br>89 | 41.5<br>29.7 | This work |
| Heulandite | HEU | 3.1x5.5<br>4.1x4.1 | 2-D | 300 | 81 | 16.2 | (Tajbakhsh et al., 2006) |
| HY | FAU | 7.4 x 7.4 | 3-D | 180 | 82 | 27.0 | (Tajbakhsh et al., 2006) |
| β-zeolite | BEA | 6.6 x 6.7<br>5.6 x 5.6 | 3-D | 300 | 39 | 7.8 | (Timofeeva et al., 2017) |
| H-ZSM-5 | MFI | 5.1 x 5.5<br>5.3 x 5.6 | 3-D | 300<br>420 | 32<br>52 | 6.4<br>6.0 | (Tajbakhsh et al., 2006; Timofeeva et al., 2017) |

[a] 0.1 mmol of (I), 0.4 mmol of acetone, 0.02 g of catalyst, 50ºC

## Figure caption

**Figure 1.** Effect of $HNO_3$ concentration on surface acidity ($pH_{ZPC}$) and Na content in AM-4. Correlation between pH and amount of samples based on AM-4 in water at 298 K.

**Figure 2.** DRIFT spectra of AM-4 pristine (1) and after modified with $HNO_3$ ((2) - 0.0625M, (3) - 0.125M, (4) - 0.25M).

**Figure 3.** DR-UV-vis spectra of AM-4 pristine (1) and after modified with $HNO_3$ ((2) - 0.0625M, (3) - 0.125M, (4) - 0.25M)

**Figure 4.** XRD patterns of AM-4 pristine and modified with 0.0625 and 0.25M $HNO_3$.

**Figure 5** Scanning electron microscope micrographs of rosette-like crystalline aggregates of AM-4

**Figure 6.** Scanning electron microscope micrographs of rosette-like crystalline aggregates of 0.25M AM-5

**Figure 7**. (A) Effect of the concentration of $HNO_3$ on the conversion of (I) and selectivities towards (II) and (III) in the presence of AM-4 samples (Experimental conditions: 0.1 mmol of (I), 0.12 mmol of acetone, 10 mg of catalyst, 4 mL of MeOH, 323 K, 120 min); (B) Dependence of yield of (III) on the surface acidity ($pH_{PZC}$) in the presence of AM-4 in reaction of cyclocondensation of (I) with acetone

**Scheme 1.** The synthesis of 1,5-benzodiazepine from 1,2-phenylenediamine and acetone.

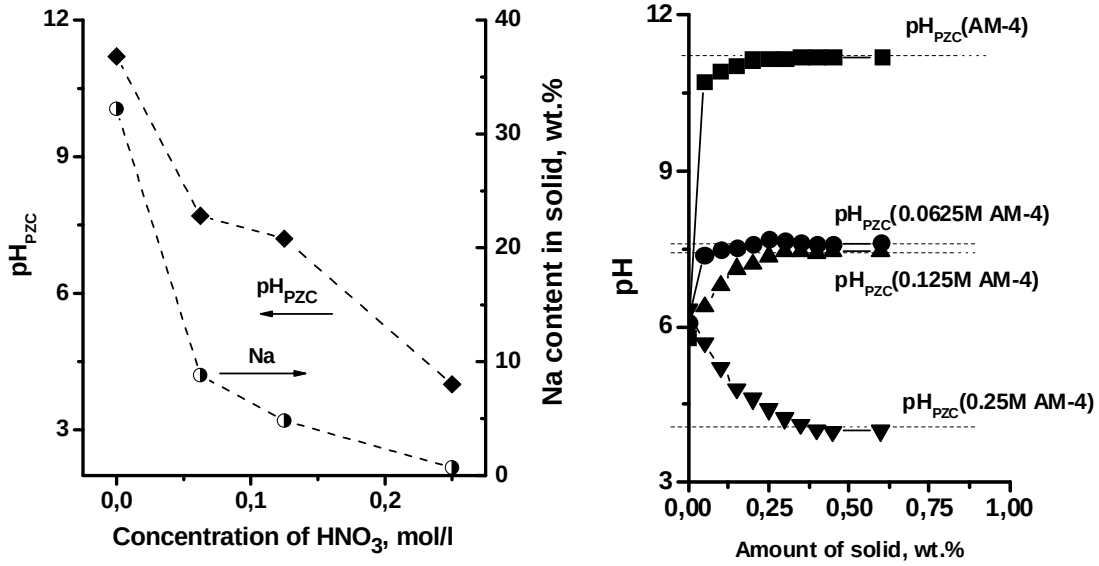


**Figure 1.** Effect of $HNO_3$ concentration on surface acidity ($pH_{ZPC}$) and Na content in AM-4. Correlation between pH and amount of samples based on AM-4 in water at 298 K.

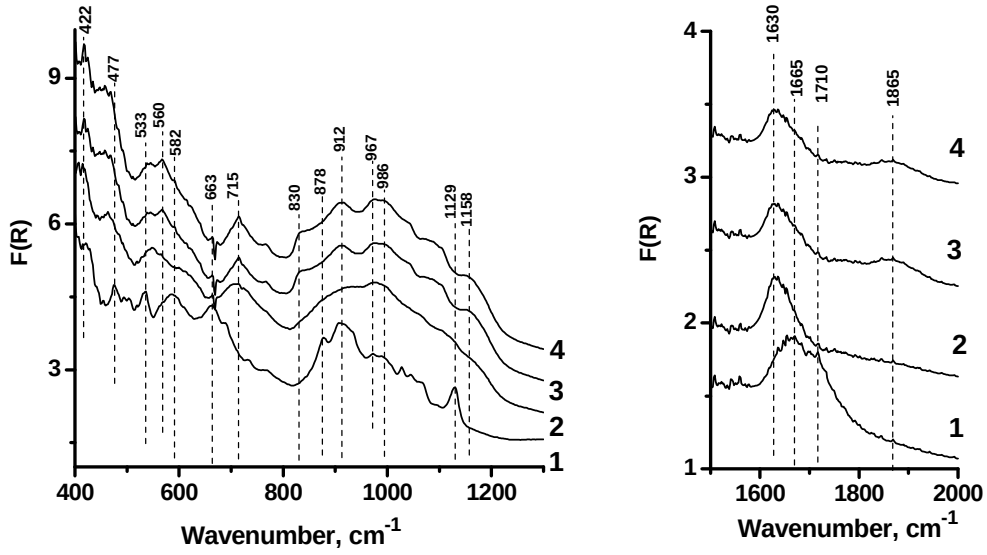


**Figure 2.** DRIFT spectra of AM-4 pristine (1) and after modified with $HNO_3$ ((2) - 0.0625M, (3) - 0.125M, (4) - 0.25M).

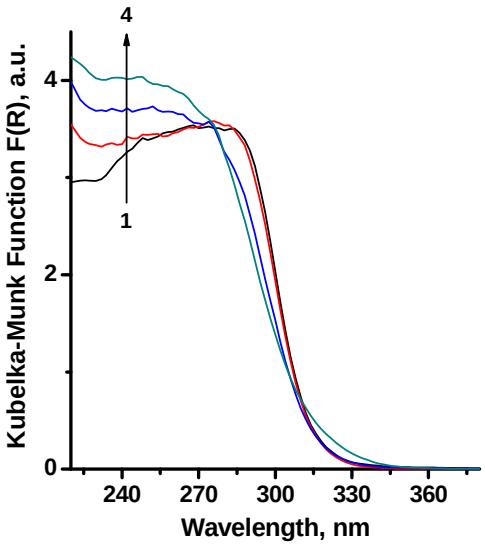


**Figure 3.** DR-UV-vis spectra of AM-4 pristine (1) and after modified with $HNO_3$ ((2) - 0.0625M, (3) - 0.125M, (4) - 0.25M)

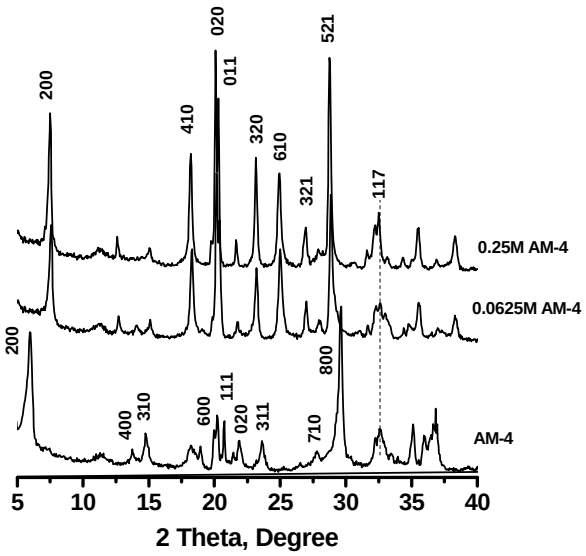


**Figure 4.** XRD patterns of AM-4 pristine and modified with 0.0625 and 0.25M $HNO_3$.

# AM-4

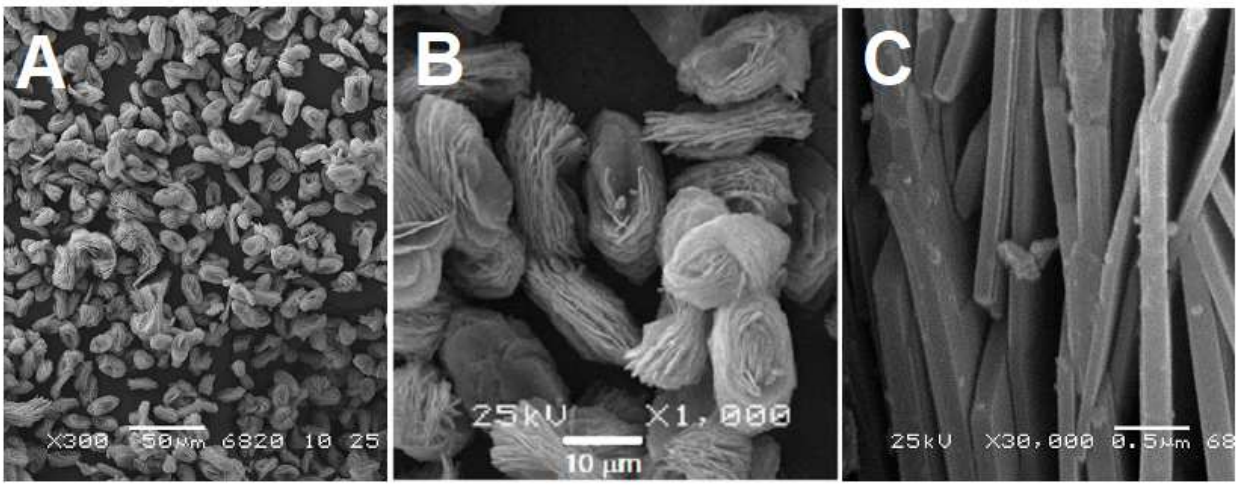


**Figure 5.** Scanning electron microscope micrographs of rosette-like crystalline aggregates of AM-4

# 0.25M AM-4

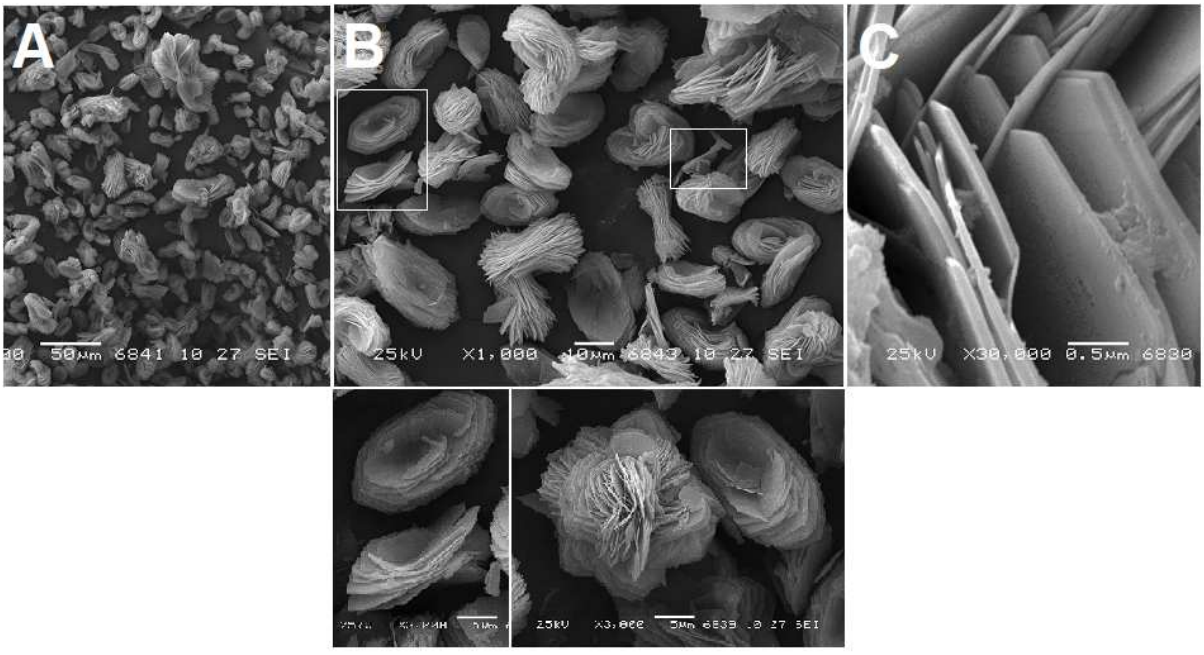


**Figure 6.** Scanning electron microscope micrographs of rosette-like crystalline aggregates of 0.25M AM-4

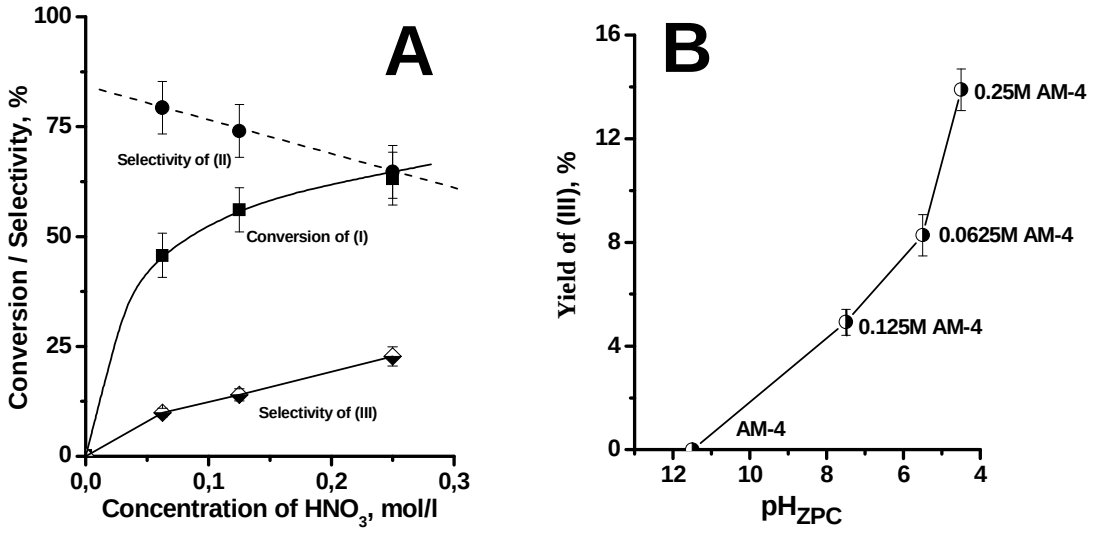


**Figure 7**. (A) Effect of the concentration of $HNO_3$ on the conversion of (I) and selectivities towards (II) and (III) in the presence of AM-4 samples (Experimental conditions: 0.1 mmol of (I), 0.12 mmol of acetone, 10 mg of catalyst, 4 mL of MeOH, 323 K, 120 min); (B) Dependence of yield of (III) on the surface acidity ($pH_{PZC}$) in the presence of AM-4 in reaction of cyclocondensation of (I) with acetone.

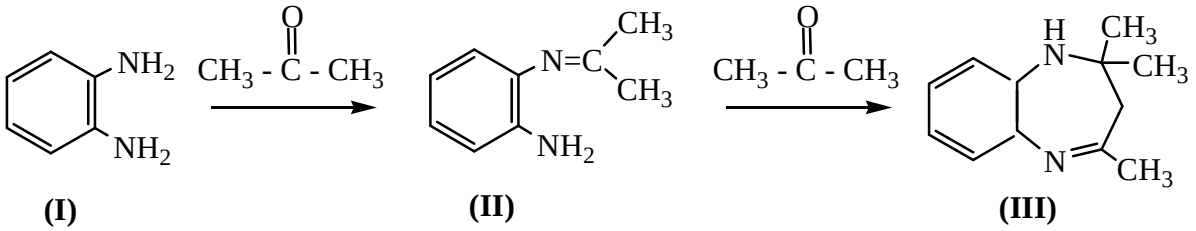


**(I)** **(II)** **(III)**

**Scheme 1.** The synthesis of 1,5-benzodiazepine from 1,2-phenylenediamine and acetone.